Effects of Adsorbent Particle Diameter on the Performance Parameters of Adsorption Chiller

Hoda Talebian [1] , Hamid Niazmand [2] , Mahdi Mahdavikhah [3]

[1]Graduate Student, Ferdowsi university of Mashhad; ho_ta708@stu-mail.um.ac.ir
[2]Assosiate Professor, Ferdowsi university of Mashhad; hniazmand@yahoo.com
[3]Graduate Student, Ferdowsi university of Mashhad; mmahdavikhah@yahoo.com

Abstract

In this analysis a plate finned-tube heat exchanger filled with SWS-1L is employed to investigate the particle diameter effect on the performance parameters of an adsorption chiller. The three dimensional heat and mass transfer equations of adsorbent bed are solved simultaneously with the heat transfer equations of thermal fluid, metal tube and fins. Both inter particle and intra particle mass transfer resistances are considered so that wide range of particle sizes can be used in the modeling process. As the effects of mass transfer resistances are concurrent, the optimum bed performance is anticipated for a specified particle diameter. Changing the geometrical parameters such as fin height and the operating parameters such as heating temperature of the thermal fluid affects the performance optimum range and the correspondent adsorbent particle diameter. Hence, it is aimed to study the effects of these parameters on the optimum particle diameter variations in detail. The results show that the cycle time and the specific cooling power have an optimum value for a specified particle diameter. This diameter increases with an increase in fin height as well as at higher heating temperature of the thermal fluid.

Keywords: adsorption chiller, numerical modeling, porous particle, mass transfer, extended surface

Introduction

Nowadays, improving energy efficiency is identified as an issue of great importance. In the field of refrigeration and air-conditioning, adsorption system is a promising technology since it incorporates environmentally benign refrigerants and the industrial waste heat or low grade solar energy instead of mechanical power. However the low value of performance parameters (COP and SCP), high initial cost and the operating pressure, which is quite lower than the atmospheric value, are the main factors that hinder the widespread application of these systems.

One of the efficient ways to improve the low SCP and COP of this system is the appropriate selection of the design and operating parameters of an adsorbent bed.

The adsorbent particles diameter is one of the influential parameters in the performance of an adsorption chiller since it simultaneously affects the intra-particle and inter-particle mass transfer resistances. Chang et.al [1] made an experimental study to investigate the effects of adsorbent layer and particle size of silica gel on the transfer processes of the adsorbent bed. They concluded that the thinner layer of adsorbent made of larger sized particles improves the mass transfer performance. Glaznev and Aristov [2] proposed an experimental study using a metal plate covered with a monolayer of loose Fuji silica gel grains with different sizes to explore the grain size effect on water sorption dynamics.

Due to the concurrent affects of inter particle and intra particle mass transfer resistances, the numerical model can be adopted safely for wide range of particle diameters only when both mentioned resistances are considered. The uniform pressure distribution approach which ignores the inter-particle mass transfer resistance is employed by some researchers in order to simplify the governing equations and to decrease the calculation time [3-5]. This approximation however is acceptable only for adsorbent beds with small thickness or large sized particles [6]. The intra-particle mass transfer resistance which is controlled by the particle porosity and the particle diameter can be neglected only for very small sized particles [7,8]. Otherwise the LDF model should be adapted to the modeling [4]. Taking into account both mass transfer resistances, Leong and Liu [9] investigated the effects of particle diameter and bed thickness as well as bed porosity and the heating temperature of thermal fluid on SCP and COP of the adsorption chiller. However, no fins were used to enhance the transfer processes and the effect of particle diameter on the system performance was not considered for different bed thicknesses, thermal fluid heating temperature or porosity. Similarly, Niazmand and Dabzadeh [10] studied the effect of particle diameter for one specified designing condition but with an exception that they used annular finned tube heat exchanger. They indicated that SCP has an optimum value with respect to particle diameter but COP is slightly dependent on particle size.

As the conductivity of adsorbent particles is relatively low, using extended surfaces can improve the heat transfer rate and consequently speeds up the adsorption and desorption rates. Although the effects of fin height and spacing on the chiller performance have been investigated earlier [10-12], it is fascinating to

study the variations of SCP and COP with particle diameter at different fin height and spacing. This study is in search to identify the specified particle diameter which corresponds to the optimum performance of the system and determine its changes at different fin heights.

Beside the geometrical parameters, the thermal fluid temperature affects the performance parameters of an adsorption chiller; therefore the influence of particle size variations on SCP and COP can be investigated for different temperatures of thermal fluid. The previous experimental studies showed that increasing the heating temperature and decreasing the cooling temperature of thermal fluid increase COP and SCP of the system [13-15]. Riffel et.al [16] numerically studied the effects of hot and cold water inlet temperature as well as chilled water inlet temperature on the performance of annular finned tube adsorbent bed with the assumptions that temperature has no variation on redial direction of the tube and the pressure is uniform throughout the bed.

As it is observed, the preceding studies did not investigate the effects of thermal fluid temperature on the particle diameter which corresponds to optimum performance of the system.

Although the previous studies clarified that the particle size affects COP and SCP of the adsorption chiller, the trend of these variations for different geometrical and operating parameters has not been studied yet. Consequently this analysis investigates the effects of fin height and the heating temperature of thermal fluid on the performance of adsorption chiller for different particle diameters with an aim to find the diameter which corresponds to the optimum performance of the system for each specified geometrical and operating condition and moreover the variation trend of this diameter with aforementioned parameters.

Description of adsorption cooling model
Figure 1 shows the schematic layout of an adsorption chiller. It comprises an adsorbent bed, a condenser, an evaporator and an expansion valve.
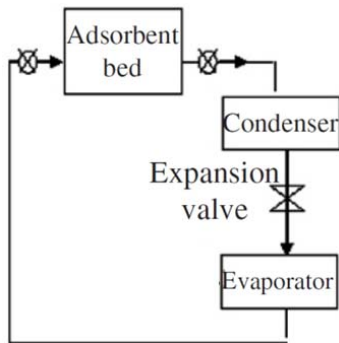

Figure 1: A schematic view of an adsorption chiller

To understand the performance of an adsorption chiller, cycle phases, which are isosteric heating, isobaric heating, isosteric cooling and isobaric cooling are described here:

In the first phase, chamber valves to condenser and evaporator are closed and the hot fluid flows through the metal tube to heat up the tube and fins. The heat is then transferred to the adsorbent to desorb the refrigerant and increase the pressure of the chamber to reach the condenser pressure due to the accumulation of the vapor in chamber. In the isobaric heating phase, heating process is continued at constant pressure by opening the valve to the condenser. The desorbed vapor is condensed at the condenser and warm condensate is allowed to flow back to the evaporator via a pressure reduction valve. Reaching a certain level of the bed average adsorbed amount, all valves are closed and the isosteric cooling phase begins. In this phase, the cold water flows through the metal tube, which reduces the temperature of the bed and the adsorption process begins. Therefore, the chamber pressure rapidly drops to the evaporator pressure. In the last phase the valve between the chamber and the evaporator is opened, while the cooling of the adsorbent is continued. The refrigeration occurs in this phase due to the continuous flow of the vapor from the evaporator to the chamber. Clearly, the continuous refrigeration can not be produced by this type of system since it is just occurred in the last phase of the working cycle. However, more continuous performance can be achieved by incorporating more than one bed in the system. [17, 18] The aforementioned phenomena are expressed mathematically using the mass and energy balances between major components of the adsorption chiller system:

1-Thermal fluid
The conservation of energy for the thermal fluid can be written as:

$$\int_{cv} \left(\rho\, C_p\right)_{fluid} \frac{\partial T_{fluid}}{\partial t} d\forall + \int_{cs} \left(\rho\, C_p\, \vec{u}\, T\right)_{fluid} . d\vec{A} =$$
$$- h_{fluid} A\left(T_{fluid} - T_{interface}\right) \qquad (1)$$

As the flow regime of the thermal fluid is commonly turbulent, the heat transfer coefficient is given by [19]

$$Nu = \frac{(f/8)\, Re\, Pr}{1.07 + 12.7(f/8)^{1/2}(Pr^{2/3}-1)} \qquad (2)$$

where f is the friction coefficient for smooth tubes, which is determined from the following correlation for the turbulent flows[19] :

$$f = (1.82 \log_{10} Re - 1.64)^{-2} \qquad (3)$$

2. Metal Tube
The transient three dimensional heat transfer equation in cylindrical coordinate is expressed by:

$$\int_{cv} \left(\rho C_p\right)_{tube} \frac{\partial T_{tube}}{\partial t} d\forall = \int_{cs} \left(\lambda\, \vec{\nabla} T\right)_{tube} . d\vec{A}$$
$$+ \gamma Q_{tube-fin} \qquad (4)$$

where the coefficient γ is set to one for the control volumes in contact with fin; otherwise it is zero.

3. Fins
Considering the negligible thickness of the fins with respect to their other dimensions, heat transfer is considered two dimensional in the plate perpendicular to the tube axis:

2

$$\int_{cv}(\rho C_p)_{fin}\frac{\partial T_{fin}}{\partial t}d\forall = \int_{cs}(\lambda_{fin}\vec{\nabla}T_{fin}).d\vec{A} - Q_{fin-b} \qquad (5)$$

4. Adsorbent Bed:

The energy balance for the adsorbent bed, neglecting viscous dissipation, is expressed as:

$$\int_{cv}\rho\, C_p \frac{\partial T_b}{\partial t}d\forall + \int_{cs}\rho_g\left(C_{pg}\vec{u}_g T_b\right)d\vec{A} = \qquad (6)$$

$$\int_{cs}\left(\lambda_b\vec{\nabla}T_b\right)d\vec{A} + \int_{cv}\rho_b\Delta H\frac{\partial w}{\partial t}d\forall$$

where ρC_p is the total heat capacity of the bed, which is determined based on the heat capacity of the dry adsorbent, gas phase, and adsorbed phase as follows:

$$\rho C_p = \varepsilon_t(\rho_g C_{pg}) + \rho_b(C_{pb} + w C_{pa}) \qquad (7)$$

where ρ_g is the gas phase density determined according to the ideal gas assumption. Porosity of the bed is given as:

$$\varepsilon_t = \varepsilon_b + (1-\varepsilon_b)\varepsilon_p \qquad (8)$$

The mass balance equation for the refrigerant is given by:

$$\int_{cv}\varepsilon_t\frac{\partial \rho_g}{\partial t}d\forall + \int_{cs}\left(\rho_g\vec{u}_g\right)d\vec{A} + \int_{cv}\rho_b\frac{\partial w}{\partial t}d\forall = 0 \qquad (9)$$

Where w is the adsorption rate calculated by:

$$\frac{dw}{dt} = 15 D_{so}\, exp\left(-\frac{E_a}{R_u T_b}\right)\Big/\left(R_p^2(w^* - w)\right) \qquad (10)$$

w^* is the equilibrium uptake at temperature T_b and the pressure P. According to [20], the following correlation has been obtained experimentally for SWS-1L:

$$w^* = \frac{1.6\times10^{-12}P\, exp\left(\frac{2.78\times10^6}{RT_b}\right)}{\left[1+\left(2\times10^{-12}P\, exp\left(\frac{2.78\times10^6}{RT_b}\right)\right)^{1.1}\right]^{1/1.1}} \qquad (11)$$

The refrigerant vapor superficial velocity is determined by Darcy correlation:

$$\vec{u}_g = -\frac{K_{app}}{\mu}\vec{\nabla}P \qquad (12)$$

Where the permeability of an adsorbent bed (K_{app}) is calculated by the following equation:

$$K_{app} = \frac{\varepsilon_b^3 d_p^2}{150(1-\varepsilon_b)^2} + \frac{\varepsilon_p\mu}{\varepsilon_b^{-0.4}P}\times$$

$$\left(\frac{1}{0.02628\frac{\sqrt{T_b^3/M}}{P\sigma^2\Omega}} + \frac{1}{29.905 d_p\sqrt{T_b/M}}\right)^{-1} \qquad (13)$$

Regarding to [21], the thermal conductivity of the adsorbent is set variable and as a function of uptake:

$$\lambda(w) = 0.1221 + 0.82w - 3.108w^2 + 4.994w^3 \qquad (14)$$

The thermal contact resistance between porous particles and heat transfer surfaces is considered according to the experimental investigation made by [22]. For particle

diameters of 0.75, 0.15 and 0.3mm the following relations are estimated respectively:

$$R_{contact\#0.075} = 0.0008 T_b^2 - 0.1214 T_b + 6.422$$

$$R_{contact\#0.15} = 0.0012 T_b^2 - 0.1624 T_b + 7.6785 \qquad (15)$$

$$R_{contact\#0.3} = 0.0013 T_b^2 - 0.1773 T_b + 8.6221$$

The relations show that the contact resistance variations decrease as the particle diameter increases. This decrement is in a way that for diameters greater than 0.3mm, we can still use the third equation with acceptable accuracy.

The equation of state is used to evaluate the density of the refrigerant vapor in desorbed phase:

$$P = \rho_g R\, T_b / M \qquad (16)$$

The chamber pressure is assumed to be equal to the condenser or evaporator pressure in isobaric phases. In isosteric phases the pressure is calculated according to the following procedure: first, the total mass flow rate of the refrigerant vapor entering the chamber is determined. Then the density is calculated from the continuity equation, and finally the chamber pressure is obtained adopting ideal gas equation of state.

The performance of adsorption chillers is mainly evaluated based on the coefficient of performance (COP), and specific cooling power (SCP), defined as:

$$COP = \frac{Q_{evap}}{Q_{in}} \qquad (17)$$

$$SCP = \frac{Q_{evap}}{m_b \times t_{cycle}} \qquad (18)$$

in which Q_{in} is the total supplied heat to the adsorbent bed by the thermal fluid during one cycle and Q_{evap} is the cooling energy produced in the evaporator:

$$Q_{in} = \int_{t_0}^{t_2}\int_{cs}(\rho C_p)_{fluid}(T_{fluid,in} - T_{fluid,out})\vec{u}_{fluid}.d\vec{A}\, dt \qquad (19)$$

$$Q_{evap} = \int_{t_3}^{t_4}\left[C_{pg}(T_{cond} - T_{evap}) - L_g\right]\dot{m}_{evap}\, dt \qquad (20)$$

where t_0 is the starting time of isosteric heating phase, t_2, t_3, and t_4 are the times needed to complete the isobaric heating, isosteric cooling and isobaric cooling phases.

The duration of isobaric heating and cooling phases are determined based on reaching a certain level of the bed average adsorbed amount. According to equations (21) and (22) the values of w^*_{max} and w^*_{min} are defined as the maximum and minimum possible bed absorbed amount at corresponding pressure of the evaporator and condenser and the cooling and heating temperatures of thermal fluid, respectively.

$$w_{min} = w^*_{min} + 0.2(w^*_{max} - w^*_{min}) \qquad (21)$$

$$w_{max} = w^*_{max} - 0.2(w^*_{max} - w^*_{min}) \qquad (22)$$

Figure 2 shows the selected computational domain of the heat exchanger based on symmetry and in order to reduce the computational cost. The spatial and temporal distributions of temperature in adsorber elements and the pressure of the adsorbent bed and the chamber are calculated by solving above equations and correlations simultaneously, taking into account the

3

appropriate initial and boundary conditions. A finite control volume method is adopted using forward differencing scheme for unsteady terms and central differencing scheme for the diffusion and convective ones. Finally an alternating direction implicit (ADI) method and the tri-diagonal solver algorithm are employed to solve the resulting discritized equations.
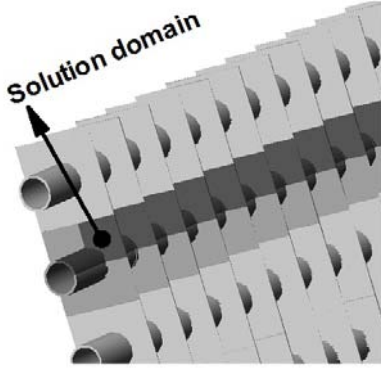

Figure 2: A schematic view of the heat exchanger computational domain

The grid independency tests have been performed to identify the optimum number of grid points. In this study, employing 16 control volumes in x direction, 16 control volumes in y direction, 8 grids between fins and 3 grids in redial direction of the tube, can satisfy the grid independency criterion for fin spacing of 6 mm and height of 8 mm. For isosteric phases, the small time step of 0.04 second is adopted due to the sharp pressure and temperature variations, while for the isobaric phases, time step of 0.4 second can provide reasonable time accurate results.

The experimental data of Restuccia et al. [23] is employed to validate the present numerical scheme with the operating and geometrical parameters adjusted to the experimental approach. For comparison, the time variations of the bed mean temperature throughout one working cycle are plotted in Figure 3, were reasonable agreements can be observed.
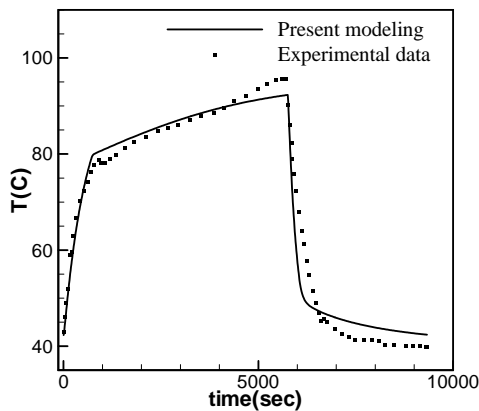

Figure 3: Comparison between numerical and experimental time variations of the bed mean temperature

All related bed specifications and chamber working conditions are listed in Table1.

Table1 : Parameters value and modeling conditions

Parameter	Symbol	Unit	Value
Inlet cold water temperature	$T_{cooling}$	K	303.15
Inlet hot water temperature	$T_{heating}$	K	358.15
Evaporator temperature	T_{cond}	K	303.15
Condenser temperature	T_{evap}	K	283.15
Adsorbent mean density	ρ_b	kgm^{-3}	650
Specific heat of adsorbent	C_{pb}	Jkg^{-1}K^{-1}	924
Heat of adsorption	ΔH	Jkg^{-1}	2.76×10^6
Inner diameter of the tube	Di	mm	10.92
Outer diameter of the tube	Do	mm	12.7
Fin thickness	FT	mm	0.2
Porosity of the particle	ε_p		0.46
Porosity of the bed	ε_b		0.36

Results and Discussion
1-Effects of adsorbent particle diameter on the performance parameters of adsorption chiller
Increasing the particle size lingers the mass transfer process inside the particle, which tends to slow down the adsorption and desorption rate in the adsorbent bed, however employing large sized particles increases the superficial velocity of the vapor due to the larger macro pore channels and thus smaller pressure gradient is expected across the adsorbent bed thickness.

Reducing particle diameter generates opposite results. Narrower macro pore channels increase the inter particle resistance which results larger pressure gradient through the bed thickness.

The preceding discussion clarifies that changing the particle diameter simultaneously affects the inter particle and intra particle mass transfer resistances in opposite directions, thus for a bed of specified configuration with fixed operating conditions, it is expected to be an optimum particle diameter at which the resultant of mass transfer resistances reaches to a minimum value. Conclusively, the desirable performance of an adsorbent bed is anticipated at this particle size. In order to verify this anticipation, performance parameters of an adsorption chiller such as cycle time, SCP and COP have been calculated for an effective range of particle diameters.
It should be noted that the system COP remains almost constant for different particle sizes. This is due to the

fact that mass transfer resistances directly affect the adsorption and desorption duration times, however, the amount of heat required for certain amount of adsorption and desorption is no time dependent. In the present study, the system COP is about 0.74 for the selected range of particle diameters when the bed specifications are the same as those reported in Table1.

Figure 4 shows the cycle time and SCP variations of an adsorption chiller as a function of particle diameter. It is observed that the cycle time has a minimum value at a specific particle diameter corresponding to minimum of both mass transfer resistances. The dominance of inter particle mass transfer resistance makes the cycle time longer for bed with particle diameter smaller than the optimum value, however this effect diminishes as the particle size increases such that for diameters larger than optimum value, the intra particle mass transfer resistance prevails over and cause the cycle time to increase. Since the cycle time conversely affects the SCP value, the optimum particle diameter corresponds to the maximum SCP as well. It must be noted that SCP is also influenced by the total adsorbent mass and cooling power, however, both are constant due to the constant porosity of the bed.
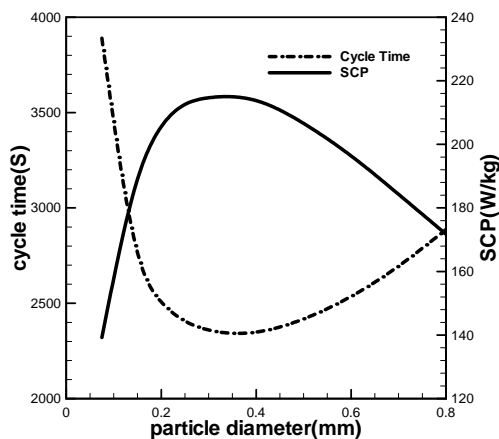

Figure 4: Cycle time and SCP variations with particle diameter (FH=8mm, FS=6mm)

Since the geometrical and operating conditions noticeably affect the performance parameters of an adsorption chiller, the effects of fin height and heating temperature of thermal fluid on the optimum particle diameter are investigated in the proceeding sections.

2-Effect of fin height on the optimum adsorbent particle diameter

At a given particle diameter, variation in fin height do not affect the intra particle mass transfer resistance. However, the inter particle resistance increases with the increase in fin height since the refrigerant vapor should travel a longer distance among the adsorbent particles, therefore the SCP of the system and also the optimum particle diameter attributed to the minimum resultant of mass transfer resistances increases as shown in Figure 5. At lower fin heights, the intra particle resistance dominates over the inter particle resistance at much lower particle diameters leading to a decrease in SCP of the system. However, at higher fin height, SCP variation

as a function of diameter is quite negligible, especially for large-sized particles. Apparently, in this situation the reduction in inter particle mass transfer resistance due to the increase in particles size compensates with the increase in intra particle resistance such that the SCP becomes independent of the particle size.
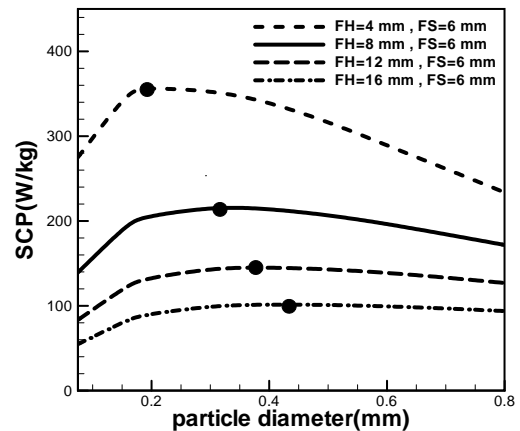

Figure 5: Variations of SCP as a function of particle diameter for different fin heights

3-Effect of thermal fluid heating temperature on the optimum adsorbent particle diameter

At a given particle diameter, increasing the heating temperature of thermal fluid directly affects the desorption rate in heating phases which increases the refrigerant mass flow rate and the cooling energy of an adsorption system. Higher refrigerant mass flow rate increases the pressure gradient through the bed which finally decreases the cycle time as shown in Figure 6. It should be mentioned that the ad/desorption range increases for higher heating temperature as the duration of isobaric heating and cooling phases are simultaneously affected by the minimum equilibrium uptake (Equation 21 and 22), however the cycle time decreases due to the high pressure gradient.
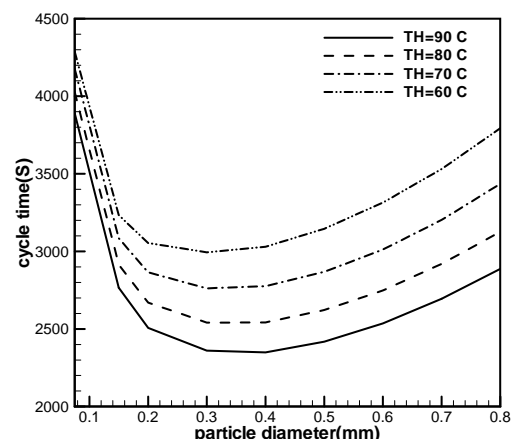

Figure 6: Variations of cycle time as a function of particle diameter for different heating temperatures of thermal fluid (FH=8mm, FS=6mm)

As a result of higher cooling energy and lower cycle time, SCP increases with an increase of the thermal fluid heating temperature (Figure 7).
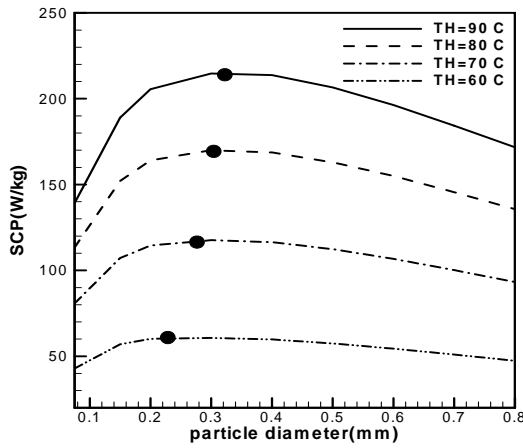
Figure 7: Variations of SCP as a function of particle diameter for different heating temperatures of thermal fluid (FH=8mm, FS=6mm)

Figure 7 shows that the optimum particle diameter, corresponds to maximum SCP and minimum cycle time, increases at higher heating temperature of thermal fluid. The reason is attributed to the high rate heat transfer that increases the pressure gradient for the optimum particle diameter range; subsequently larger particles are needed to provide the required macro-pore channels. The variation range of the optimum particle diameter is about 0.09mm for 30C increase in the heating temperature.

Considering Figure 6, another challenging issue is that for very small particle diameters the cycle time is slightly dependent on the heating temperature but for large sized particles this dependency is noticeable. The reason is that for very small particle diameters the inter particle mass transfer resistance is dominant and too strong to be influenced by the increasing power of refrigerant flow at higher temperatures thus the cycle time remains nearly unchanged. However, for larger particles the increasing rate of intra particle resistance is conversely influenced by higher desorption rate at higher bed temperatures. Therefore the cycle time increases with a slower rate as compared to lower heating temperatures.

Conclusions

This study investigates the effects of adsorbent particle diameter on the performance parameters of an adsorption chiller for different geometrical and operational conditions of the adsorbent bed. The three dimensional numerical modeling which considers the spatial variations of pressure and gas flow inside the bed as well as the internal and external resistances of bed particles is adopted and developed. The results show that the cycle time has a minimum value at the specific particle diameter which corresponds to the maximum specific cooling power of the system. This optimum diameter is influenced by different parameters such as fin height and heating temperature of the thermal fluid. The optimum particle size increases with an increase in fin height and also at higher heating temperature of thermal fluid.

List of Symbols

E_a	Activation energy (Jkg^{-1})
$R_{contact}$	Contact resistance(m^2KW^{-1})
FH	Fin Height (m)
FS	Fin space (m)
f	Friction factor
R	Gas constant($Jkg^{-1}K^{-1}$)
M	Molar mass($kgmol^{-1}$)
Pr	Prandtl number
D_{so}	Pre-exponent constant of surface diffusivity(m^2s^{-1})
P	Pressure (Pa)
Re	Reynolds number
t	Time(s)
R_u	Universal gas constant($Jmol^{-1}K^{-1}$)
u	Velocity (ms^{-1})

Greek symbols

Ω	Collision integral
σ	Collision diameter for Lennard-Jones potential(A)
μ	Viscosity (Pa.s)
λ	Thermal conductivity ($Wm^{-1}K^{-1}$)

Subscripts

a	Adsorbate
b	Adsorbent
g	Vapor

References
[1] Chang, K.S., Chen, M.T., Chung, T.W., 2005. "Effects of the thickness and particle size of silica gel on the heat and mass transfer performance of a silica gel-coated bed for air-conditioning adsorption systems". *Appl. Therm. Eng*, 25(14-15),October, pp. 2330-2340.
[2] Glaznev, I.S., Aristov, Y.I., 2010. "The effect of cycle boundary conditions and adsorbent grain size on the water sorption dynamics in adsorption chillers". *Int. J. Heat Mass Transf*, 53(9-10), April, pp. 1893-1898.
[3] Chua, H.T., Ng, K.C., Wang, W., Yap, C., Wang, X.L., 2004. "Transient modeling of a two-bed silica gel-water adsorption chiller". *Int. J. Heat Mass Transf*, 47(4), February, pp. 659-669.
[4] Di, J., Wu, J.Y., Xia, Z.Z., Wang, R.Z., 2007. "Theoretical and experimental study on characteristics of a novel silica gel-water chiller under the conditions of variable heat source temperature". *Int. J. Refrigeration*, 30(3), May, pp. 515-526.

[5] Miyazaki, T., Akisawa, A., Saha, B.B., El-Sharkawy, I.I, Chakraborty, A., 2009. "A new cycle time allocation for enhancing the performance of two-bed adsorption chillers". *Int. J. Refrigeration*, 32(5), August, pp. 846-853.

[6] Yong, L., Sumathy, K., 2004. "Comparison between heat transfer and heat mass transfer models for transportation process in an adsorbent bed". *Int. J. Heat Mass Transf*, 47(8-9), April, pp. 1587-1598.

[7] Amar, N.B., Sun L.M., Meunier, F., 1996. "Numerical analysis of adsorptive temperature wave regenerative heat pump". *Appl. Therm. Eng*, 16(5), May, pp. 405-418.

[8] Marletta, L., Maggio, G., Freni, A., Ingrasciotta, M., Restuccia, G., 2002. "A non-uniform temperature non-uniform pressure dynamic model of heat and mass transfer in compact adsorbent beds". *Int. J. Heat Mass Transf*, 45(16), July, pp. 3321-3330.

[9] Leong, K.C., Liu, Y., 2004, "Numerical modeling of combined heat and mass transfer in the adsorbent bed of a zeolite/water cooling system". *Appl. Therm. Eng*, 24(16), November, pp. 2359-2374.

[10] Niazmand, H., Dabzadeh, I., 2012. "Numerical simulation of heat and mass transfer in adsorbent beds with annular fins". *Int. J. Refrigeration*, 35(3), May, pp. 581–593.

[11] Kubota, M., Ueda, T., Fujisawa, R., Kobayashi, J., Watanabe, F., Kobayashi, N., Hasatani, M., 2008. "Cooling output performance of a prototype adsorption heat pump with fin-type silica gel tube module". *Appl. Therm. Eng*, 28(2-3), February, pp. 87-93.

[12] Rezk, A.R.M., Al-Dadah, R.K., 2012. "Physical and operating conditions effects on silica gel/water adsorption chiller performance". *Appl. Energy*, pp. 89(1), January, 142-149.

[13] Chang, W.S., Wang, C.C., Shieh, C.C., 2007. "Experimental study of a solid adsorption cooling system using flat-tube heat exchangers as adsorption bed". *Appl. Therm. Eng*, 27(13), September, pp. 2195-2199.

[14] Freni, A., Sapienza, A., Glaznev, I.S., Aristov, Y.I., Restuccia, G., 2012. "Experimental testing of a lab-scale adsorption chiller using a novel selective water sorbent "silica modified by calcium nitrate" ". *Int. J. Refrigeration*, 35(3), May, pp. 518–524.

[15] Luo, H., Wang, R., Dai, Y., 2010. "The effects of operation parameter on the performance of a solar-powered adsorption chiller". *Appl. Energy*, 87(10), October, pp. 3018-3022.

[16] Riffel, D.B., Wittstadt, U., Schmidt, F.P., Núñez, T., Belo, F.A., Leite, A.P.F., Ziegler, F., 2010. "Transient modeling of an adsorber using finned-tube heat exchanger". *Int. J. Heat Mass Transf*, 53(7-8), March, pp. 1473-1482.

[17] Chua, H.T., Ng, K.C., Wang, W., Yap, C., Wang, X.L., 2004. "Transient modeling of a two-bed silica gel-water adsorption chiller". *Int. J. Heat Mass Transf*, 47(4), February, pp. 659-669.

[18] San, J.Y., Hsu, H.C., 2009. "Performance of a multi-bed adsorption heat pump using SWS-1L composite adsorbent and water as the working pair". *Appl. Therm. Eng*, 29(8-9), June, pp. 1606–1613.

[19] Poyelle, F., Guilleminot, J., Meunier, F., 1999. "Experimental tests and predictive model of an adsorptive air conditioning unit". *Ind. Eng. Chem. Res*, 38(1), pp. 298–309.

[20] Saha, B.B., Chakraborty, A., Koyama, S., Aristov, Y.I., 2009. "A new generation cooling device employing CaCl2-in-silica gel-water system". *Int. J. Heat Mass Transf*, 52(1-2), January, pp. 516–524.

[21] Freni, A., Tokarev, M.M., Restuccia, G., Okunev, A.G., Aristov, Y.I., 2002. "Thermal conductivity of selective water sorbents under the working conditions of a sorption chiller". *Appl. Therm. Eng*, 22(14), October, pp. 1631-1642

[22] Zhu, D., Wang, S., 2002. "Experimental investigation of contact resistance in adsorber of solar adsorption refrigeration". *Solar energy*, 73(3), September, pp. 177-185.

[23] Restuccia, G., Freni, A., Vasta, S., Aristov, Y., 2004. "Selective water sorbent for solid sorption chiller: experimental results and modeling". *Int. J. Refrigeration*, 27(3), May, pp. 284-293.